The Korean Journal of Ceramics, **5** [2] 131 - 136 (1999)

Deposition of Yttria Stabilized Zirconia by the Thermal CVD Process

In Deok Jeon†, Latifa Gueroudji* and Nong M. Hwang†*

†*National Creative Initiative Center for Microstructure Science of Materials*
Seoul National University, Seoul 151-742, Korea
**Korea Research Institute of Standards and Science, P.O. Box 102,*
Taejon 305-600, Korea
(Received September 23 1998)

Yttria stabilized zirconia (YSZ) films were deposited on porous NiO substrates and quartz plates by the thermal CVD using $ZrCl_4$, YCl_3 as precursors, and O_2 as a reactive gas at atmospheric pressure. The evaporation temperature of $ZrCl_4$ was varied from 250°C to 550°C while the temperatures of YCl_3 and the substrate were varied from 1000°C to 1030°C. As the evaporation temperature of $ZrCl_4$ increased, the deposition rate of ZrO_2 decreased, contrary to our expectation. As a result of the decreased deposition rate of ZrO_2, the yttria content increased. The high evaporation temperature of $ZrCl_4$ makes the well-faceted crystal while the low evaporation temperature leads to the cauliflower-shaped structure. The dependence of the evaporation temperature on the growth rate and the morphological evolution was interpreted by the charged cluster model.

Key words : YSZ, Charge cluster model, Porous substrate, Morphology, Thin film, Cauliflower

I. Introduction

YSZ is one of attractive materials for solid electrolyte due to its high oxygen ion conductivity. The efficiency of a solid oxide fuel cell depends on ion resistance of the solid electrolyte. Thickness of the electrolyte is a main factor deciding the efficiency and thus, minimization of the thickness is required to increase the efficiency. So intensive efforts have been made to decrease the thickness.[1-10] YSZ films have been deposited on nonporous substrates such as silicon and quartz by thermal CVD using chlorides as precursors.[1] However, deposits on porous substrates by CVD have no gas-tight dense films. EVD (electrochemical vapor deposition) have been known as the promising process that can deposit the gas-tight thin YSZ film on porous substrate for the electrolyte.[2-10] However, EVD has a disadvantage in production cost. Many efforts are being made for development of the cost effective and the reliable zirconia film for the electrolyte in SOFC (solid oxide fuel cell) application.

In order to overcome the difficulties encountered in the thin film process by CVD and to make a breakthrough, the growth mechanism of the zirconia film in the CVD process should be clarified. On the other hand, Hwang et al[11] suggested the charge cluster model as the growth mechanism of the CVD diamond process. According to our analysis, this growth mechanism is quite general in the CVD process. It is highly probable that the growth of the ZrO_2 film in the CVD process should be by the charged clusters.

In the charged cluster model, the deposition is the two-step process: nucleation in the gas phase and the growth by these nuclei. The nuclei are charged and their size is nanometer and invisible. The growth of the charged clusters is inhibited by the Coulomb repulsion. Therefore, the size of the clusters depends on the charge density.

In the case of the thermal CVD, the nucleation is induced by ions. It should be reminded that in the Wilson cloud chamber experiment on nucleation from the water vapor, the formation of the charged cluster by ion-induced nucleation was unavoidable even in the clean room-temperature air.[12-14] Later it was realized that ions were continuously generated even in clean room-temperature air by natural radioactivity and cosmic rays. This is how natural radioactivity and cosmic rays were discovered.

We could confirm that in the thermal CVD process, more than nano-ampere current is measured when the reactant gases decompose in the reactor. The generation of ions is presumed to be chemionization during the chemical reactions among the gas species. Since one ampere is the flux of $\sim 10^{19}$ ions per second, nanoampere is the flux of $\sim 10^{10}$ ions per second, which is much larger than the number density of ions in the clean room-temperature air. Considering that even in the clean room-temperature air the ion-induced nucleation was unavoidable, the ion-induced nucleation during the thermal CVD process is highly probable in the presence of the appreciable supersaturation for precipitation. When the clusters or tiny particles in the gas phase are in the nanometer size, they are invisible; the objects are invisible if they are smaller than the minimum wavelength of the visible light, which is ~500 nm.

According to Fujita,[15-17] the clusters of nanometer size have an unusual property. These clusters behave like

liquid in their ability of deformation and diffusion because of lack in the long-range interaction. Because of this unusual property, atom clusters undergo sintering at room temperature and can make an epitaxial film as well as a polycrystalline one. Fujita found out that the transition between fast-diffusion liquid-like and slow-diffusion crystalline properties takes place abruptly with size of the clusters, which he called a magic size. The magic size for the embodied ZrO_2 was determined to be ~6 nm at room temperature by Fugita.[16] The magic size for the isolated state is expected to be ~12 nm. Moreover, the magic size of the ZrO2 clusters in the CVD reactor at the deposition temperature of 1000°C is expected to be larger than ~12 nm.

The growth by charged clusters has some characteristics. When the charge density is high, the cluster size becomes small. As the size of the charged cluster gets small, the Coulomb repulsion is dominant between the clusters and the growing surface especially in the case of the film with poor electrical conductivity. As a result, the growth rate tends to be low although the small cluster size together with the slow flocculation property makes the nicely-faceted film. As the size of the charged cluster gets large, however, van der Waals attraction is dominant between the clusters and the growing surface. And the growth rate tends to be high although the large cluster size together with the fast flocculation property makes the cauliflower-shaped film. These features are clearly revealed in the diamond and silicon CVD processes.

Another important feature in the growth by the charged clusters is the deposition behavior depends on the substrate. The charged clusters easily land on the conducting substrate while they have difficulty in landing on the insulating substrate. As a result, the growth rate on the conducting substrate is much faster than that on the insulating substrate in the initial stage. Besides, the substrate with the high charge transfer rate tends to make the soot-like porous film while the substrate with the low charge transfer rate tends to make the dense film.

In this paper, the possibility of thin YSZ film deposition on porous NiO substrates by thermal CVD will be presented. The effects of the temperature of precursors on the growth rate, the yttria content and the morphology were studied and interpreted from the viewpoint of charged cluster model. Analyses of the films were done by SEM (scanning electron microscopy)/EDS (energy dispersive spectroscopy), EPMA (electron probe micro-analyzer) and XRD (X-ray diffraction).

II. Supersaturation ratio for ZrO_2 deposition in Zr-Cl-O system

The driving force for precipitation of a solid from gas phase in CVD can be determined by the supersaturation ratio which is defined as the ratio of the partial pressure of the species to deposit in the gas phase equilibrium to its equilibrium vapor pressure.[18] With this scheme, the supersaturation ratio for precipitation of zirconia in the Zr-Cl-O system is calculated by Themo-Calc software.

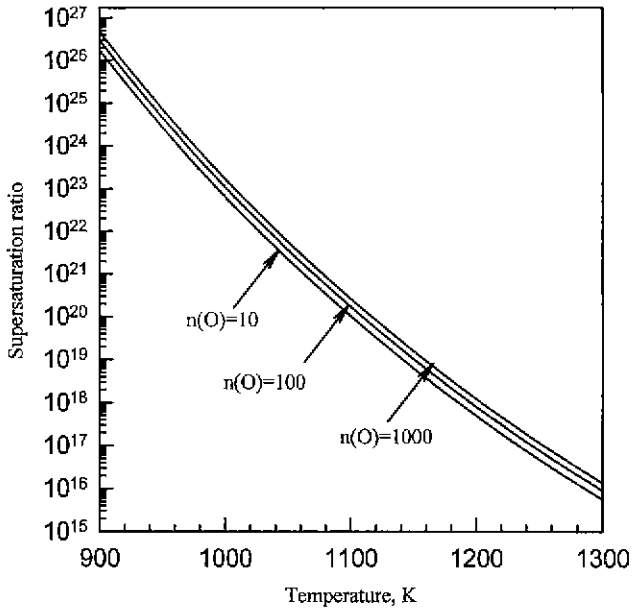

Fig. 1. Supersaturation ratio of ZrO_2 with temperature in the Zr-Cl-O system: P=101325 Pa, n(Zr)=1 and n(Cl)=4.

Fig. 1 shows the supersaturation ratio of ZrO_2 versus temperature in the condition of n(Zr)=1, n(Cl)=4 and P= 101325 Pa, where 'n' represents the number of mole. The supersaturation ratio increases with temperature and is higher than 10^{16} in all temperature range of 900~1300 K. In this highly supersaturated state, the gas phase nucleation of ZrO_2 will take place and the nuclei, whose electron affinity and ionization potential approaches the work function value, will be charged.

III. Experimental Procedure

The schematic diagram of the CVD reactor is shown in Fig. 2. $ZrCl_4$(99.9%, Aldrich) and YCl_3(99.9%, Aldrich)

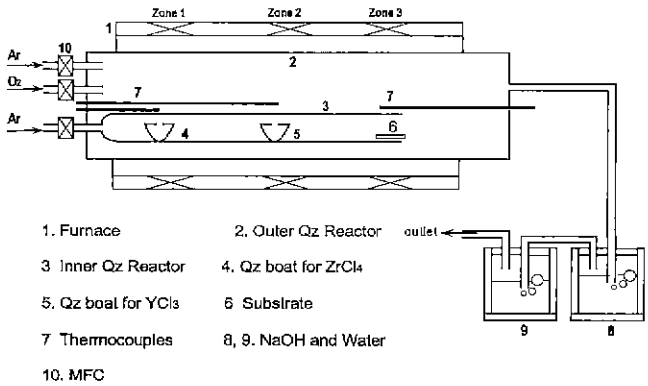

Fig. 2. Schematic diagram of the CVD reactor for the YSZ film deposition by thermal CVD.

Table I. Experiment Conditions and EPMA Data

Temperature $ZrCl_4$ (°C)	Temperature YCl_3 (°C)	Temperature substrate (°C)	Time (hrs)	Mol % of Y_2O_3 (+/-2%) by EPMA
550	1000	1000	2	25
450	1000	1000	1.5	15
400	1000	1000	1.5	12
320	1030	1030	2	13
300	1000	1000	2	4
250	1020	1020	2	2

powders were used as precursors. And oxygen was used as reactive gas. A 3-zone tube furnace was used. The temperatures of substrates and YCl_3 were controlled within ±5°C and that of $ZrCl_4$ was within ±20°C. $ZrCl_4$ was heated to 250~550°C, YCl_3 was to 1000~1030°C and the substrate was to 1000~1030°C. The YCl_3 precursor and the substrate were placed at the site of the same temperature. The distance between the $ZrCl_4$ precursor and the substrate was ~50 cm along the tube. Porous NiO substrates were prepared by sintering pallets of Ni powder at 1000°C for 5 hrs. The flow rate of Ar for carriage of precursors in the inner tube was 100 sccm. The flow rates of O_2 and Ar in the outer tube were 100 and 30 sccm, respectively. Chlorine gas is formed by reactions inside the reactor. The NaOH solution was used for trapping the chlorine gas as shown Fig. 2. The condition for deposition is in Table I.

In order to study the influence of the substrate materials on the film morphology, which was attributed to a critical factor in the evolution of film morphology according to the charged cluster model,[11] the porous NiO and the quartz substrates were placed next to each other under the same processing condition and the microstructrual evolution was compared. The growth rate of the films was estimated by SEM (Akashi ISI DS-130C) of cross-section of the YSZ films. The Y_2O_3 content in the films was measured by EPMA (Cameca SX-50). The morphology was studied by SEM and EDS (Phillips PV9900). XRD (Rigaku RPT 300) was used for phase analyses.

IV. Results

1. Growth rate of ZrO_2 and Y_2O_3 content with the $ZrCl_4$ temperature

The growth rate of the film decreased as the temperature of $ZrCl_4$ increased in the range 250-550°C. The growth rate was ~1 μm/hr in the $ZrCl_4$ temperature range of 400-550°C. The growth rate was in the range of 5-10 μm/hr in the $ZrCl_4$ temperature range of 250-350°C. These results indicate that the growth rate of ZrO_2 decreased with increasing vapor pressure of $ZrCl_4$. This aspect is unusual because the high deposition rate is expected from the high evaporation rate.

According to the phase diagram of ZrO_2-Y_2O_3, 8~38 mol% Y_2O_3 is required for the single phase of cubic zirconia at 1000°C. The fraction of Y_2O_3 in the ZrO_2 film typically used for the solid electrolyte is 8-12 mol%. The Y_2O_3 content of the films was 2-25 mol% (Table I). 12 mol%, of Y_2O_3 was obtained at T_{ZrCl4}=400°C, T_{YCl3}=1000°C, and T_{sub}=1000°C (Table I). The Y_2O_3 content was varied sensitively with the temperature of the $ZrCl_4$ precursor. The phase of the films was cubic YSZ or cubic YSZ mixed with a little monoclinic ZrO_2 (Fig. 3). The content of Y_2O_3 in the film increased as the temperature of the $ZrCl_4$ precursor increased with the temperature of YCl_3 and the substrate fixed at ~1000°C. This means that the amounts of ZrO_2 in the films decreased as the temperature of $ZrCl_4$ increased.

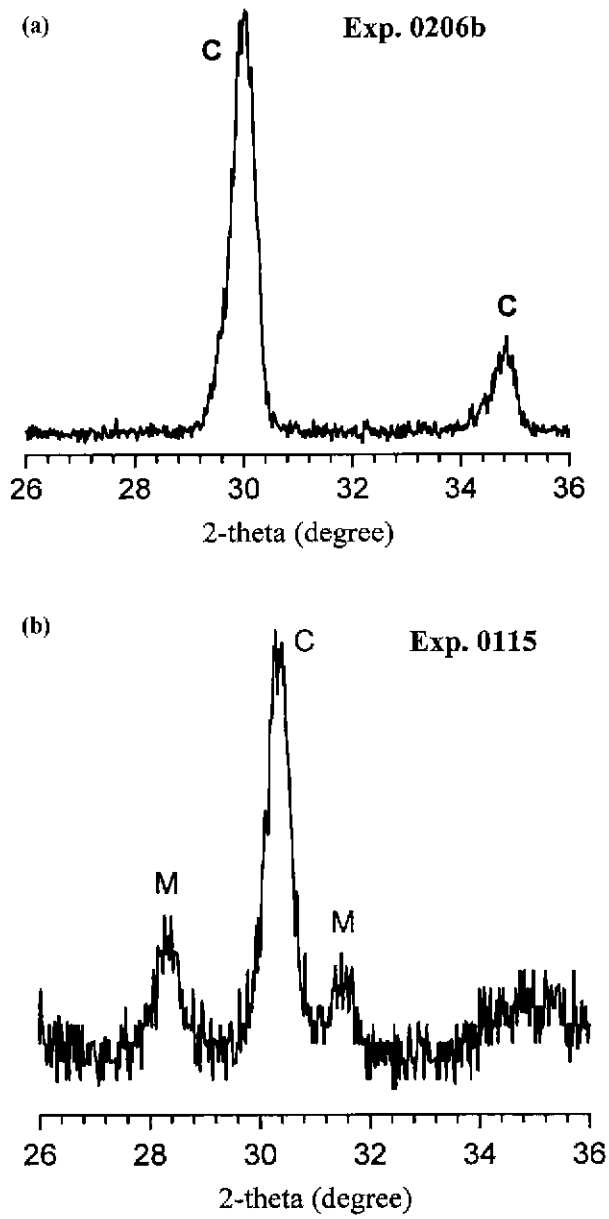

Fig. 3. XRD spectrum of YSZ films deposited on NiO substrate at (a); T_{ZrCl4}=320°C, T_{YCl3}=1000°C, T_{sub}=1000°C for 2 hrs and (b); T_{ZrCl4}=400°C, T_{YCl3}=1000°C, T_{sub}=1000°C for 1.5 hrs.

Fig. 4. SEM of the YSZ film deposited on a porous NiO substrate at T_{ZrCl4}=450°C, T_{YCl3}=1000°C and T_{sub}=1000°C for 1 5 hrs.

2. Morphology of films

The films with well-developed facets tended to develop at the high temperature of the $ZrCl_4$ precursor, while the film morphology resembling the cauliflower tended to develop at the low temperature. Fig. 4 shows the SEM microstructure of the film deposited on the porous NiO substrate at T_{ZrCl4}=450°C, T_{YCl3}=1000°C and T_{sub}=1000°C. The microstructure shows the relatively large grains of ~5 μm with well-developed facet. In the microstructure, small particles of 0.1 μm are observed on the surface of the film. They appear white and some of them are in aggregates. Analysis by EDS indicates that they are zirconia. These particles seems to have landed on the surface from the gas phase after the temperature of the reactor was turned off.

Fig. 5 shows cauliflower-shaped films deposited on the porous NiO substrate at T_{ZrCl4}=250°C, T_{YCl3}=1020°C and T_{sub}=1020°C. While each grain of ~5 μm in Fig. 4 is single crystalline, each spherical lump of ~5 μm in Fig. 5 is polycrystalline, consisting of numerous tiny submicron grains. The growth rate of the cauliflower-shaped films in Fig. 5 was 5~10 times higher than that of the films with well-developed facets in Fig. 4.

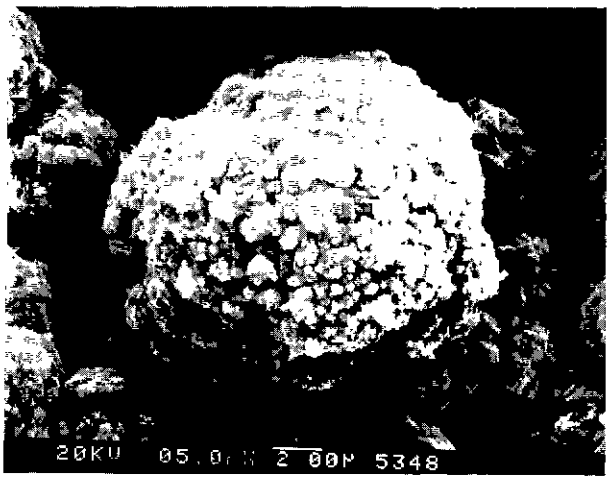

Fig. 5. SEM of the YSZ film deposited on a porous NiO substrate at T_{ZrCl4}=250°C, T_{YCl3}=1020°C and T_{sub}=1020°C for 2 hrs.

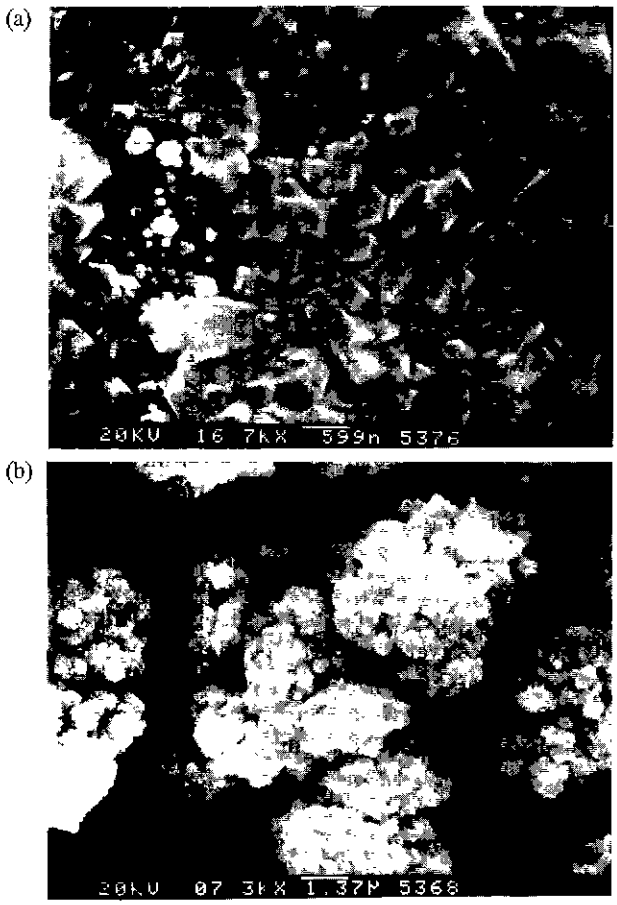

Fig. 6. SEM of the YSZ film deposited, at T_{ZrCl4}=320°C, T_{YCl3}=1030°C, T_{sub}=1030°C for 2 hrs., (a) on a quartz plate and (b) on a porous NiO substrate.

3. Effect of the substrate materials on morphology

Two different substrates of quartz and porous NiO were placed next to each other and deposited for the condition of T_{ZrCl4}=320°C, T_{YCl3}=1030°C and T_{sub}=1030°C. The film deposited on the quartz substrate shows the well-developed facets and is relatively dense (Fig. 6(a)) while the film on the NiO substrate shows a typical cauliflower structure and is porous (Fig. 6(b)). The growth rate on the quartz substrate (less than ~0.2 μm/hr) was roughly 20 times lower than that on the NiO substrate.

V. Discussion

In the films, the Y_2O_3 content increased with the temperature of $ZrCl_4$ at the fixed temperature of YCl_3 at ~1000°C. Since the temperature of YCl_3 is fixed, the flux of Y_2O_3 into the film will be constant. Therefore, the

higher content of Y_2O_3 indicates that the flux of ZrO_2 into the film decreased. The higher content of Y_2O_3 and the low growth rate of the film with increasing vaporizing temperature of $ZrCl_4$ are contrary to our expectation that increasing vaporizing pressure of $ZrCl_4$ would result in the larger flux of ZrO_2 into the film or the higher growth rate of the film.

We will explain this aspect by the charged cluster model as mentioned in the introduction. The low growth rate for the high evaporation temperature of $ZrCl_4$ indicates that the cluster size is smaller while the high growth rate for the low evaporation temperature indicates that the cluster size is larger. Since the cluster size decreases with increasing charge density, the high evaporation temperature seems to produce the high charge density. Since the amount of charge produced during the decomposition of the reactant gases will be proportional to the evaporation temperature of $ZrCl_4$, the higher evaporation temperature will produce the larger charge density. According to our analysis, the size of the cluster is inversely proportional to the square of the charge density. Considering the increase in the amount of precipitation by the high evaporation temperature, the size of the cluster would be inversely proportional to the charge density. Therefore, the high evaporation temperature results in the low growth rate, the high yttria content and the well-faceted morphology as shown in Fig. 4. However, the low evaporation temperature results in the high growth rate, the low yttria content and the cauliflower morphology as shown in Fig. 5. The cauliflower structure indicates that the nanoclusters tend to retain their individual orientation because they frequently fail in the epitaxial recrystallization. Since the magic size of the isolated ZrO_2 is expected to be a little larger than 12 nm based on Fujita's result,[15] the clusters much larger than 12 nm will make the cauliflower structure.

Here, the growth rate decrease with increasing precursor temperature is attributed to the accompanied increase of the charge density, which is confirmed by our current measurement. This conclusion is valid only when the effect of the increase in the charge density outweighs the effect of increasing evaporation flux. And the conclusion might be valid especially when we use the solid precursors, which have relatively highly evaporation temperatures. It should be noted that in general the growth rate increases with the flow rate of reactant gases or the evaporation temperature of liquid precursors,[19-20] in which case the precursor temperatures are relatively low and at such low temperatures, the precursors just vaporize without decomposition. And the effect of the increase in the charge density might not outweigh the effect of the increasing vapor flux.

On the other hand, quite often in the MOCVD process, the cauliflower structure changed to the crystal with well-defined facets with the marked decrease of the growth rate when the substrate temperature increases above some values.[21] The low growth rate has been attributed to the onset of the gas phase nucleation.[22] We believe that such transition in the deposition behavior with increasing substrate temperature might be attributed to the increase in the charge density as in the case of our present experiment.

The charged cluster model can also be applied to the dependence of the morphology on the substrates. In the model, the film morphology is affected by the rate that the cluster loses its charge at the substrate. When the charged cluster approaching the substrate loses its charge quickly to the substrate, it becomes neutral and tends to land on the growing surface by random Brownian coagulation, promoting a cauliflower structure. When the charged cluster loses its charge relatively slowly to the substrate, it will land selectively on the macro kink site and the epitaxial sticking of the cluster on the growing surface is promoted. As a result, the evolution of the relatively dense crystalline film with the well-developed facets is favored. Therefore, the substrates with high and low charge transfer rates will promote, respectively, the cauliflower structure and the dense film. However, the growth rate would be higher for the substrate with a high charge transfer rate.

Ni has a high charge transfer rate. Although the data for the charge transfer rate of NiO is not available, NiO is known to have a high catalytic effect. Therefore, NiO is expected to have a charge transfer rate much higher than quartz, which is insulating. The substrate effect shown in Fig. 6 is in good agreement with this suggestion. The growth rate of the film on NiO was ~20 times higher than that of on quartz.

VI. Conclusion

With increasing the vaporizing temperature of $ZrCl_4$, the yttria content increased, the growth rate of film decreased and the film of crystals with well-developed facets was evolved. On the other hand, the cauliflower structure was evolved at the low temperature of $ZrCl_4$. These results were interpreted based on the charged cluster model; the high vaporizing temperature of $ZrCl_4$ produces the high ion density, resulting in small charged clusters of ZrO_2, which are responsible for the low growth rate and for the evolution of crystals with well-developed facets. The porous cauliflower structure was evolved on the NiO substrate, while the relatively dense film with well-developed facets was on the quartz substrate in the same processing condition. This substrate effect was attributed to the difference in the charged transfer rate of the two substrates.

Acknowledgment

This work was supported by Korea Electric Power Research Insitute. Additional support was provided by

National Creative Initiative Center for Microstructure Science of materials.

References

1. T. Hirai and H. Yamane, "Yttria- Stabilized Zirconia Transparent Films Prepared by Chemical Vapor Deposition," *J. Crystal. Growth*, **94**, 880-884 (1989).
2. G. Z. Cao, H. W. Brinkman, J. Meijerink, K. J. de Vries and A. J. Burggraaf., "Pore Narrowing and Formation of Ultrathin Yttria-Stabilized Zirconia Layers in Cramic Membranes by Chemical Vapor Deposition/Electrical Vapor Deposition," *J. Amer. Ceram. Soc.*, **76**(9), 2201-2208 (1993).
3. J. Schoonman, J. P. Dekker, J. W. Broers and N. J. Kiwiet, "Electro Chemical Vapor Deposition of Stabilized Zirconia and Interconnection Materials for Solid Fuel Cells," *Solid State Ionics*, **46**, 299-308 (1991).
4. L. G. J. de Haart, Y. S. Lin, K. J. de Vries and A. J. Burggraaf, "Modified CVD of Nanoscale Structures in and EVD of Thin Layers on Porous Ceramic Membranes," *J. Europ. Ceram. Soc.*, **8**, 59-70 (1991).
5. L. G. J. de Haart, Y. S. Lin, K. J. de Vries and A. J. Burggraaf, "On the Kinetic Study of Electrocehemical Vapor Deposition," *Solid State Ionics*, **47**, 331-336 (1991).
6. L. G. J. de Haart, Y. S. Lin, K. J. de Vries and A. J. Burggraaf, "A Kinetic Study of the Electrochemical Vapor Deposition of Solid Oxide Electrolyte Films on Porous Substrates," *J. Electrochem. Soc.*, **137**(12), 3961-3967 (1990).
7. U. B. Pal and S. C. Singhal, "Electrochemicl Vapor Deposition of Yttria-Stabilized Zirconia Films," *J. Electrochem. Soc.*, **137**(9), 2937-2941 (1990).
8. M. F. Carolan and J. N. Michaels, "Growth Rate and Mechanism of Electrochemical Vapor Deposited Yttria Stabilized Zirconia Films," *Solid State Ionics*, **37**, 189-195 (1990).
9. M. F. Carolan and J. N. Michaels, "Morphology of Electrochemical Vapor Deposited Yttria Stabilized Zirconia Films," *Solid State Ionics*, **37**, 197-202 (1990).
10. M. F. Carolan and J. N. Michaels, "Chemical Vapor Deposited Yttria Stabilized Zirconia on Porous Support," *Solid State Ionics*, **25**, 207-216 (1987).
11. N. M. Hwang, J. H. Hahn and Duk Y. Yoon, "Charged Cluster Model in the low Pressure Synthesis of Diamond," *J. Crystal growth*, **162**, 55-68 (1996).
12. C. T. R. Wilson, "Cloud-chamber Technique," *Proc. Roy. Soc.* **85**, 285 (1911).
13. C. T. R. Wilson, "Cloud-chamber Technique," *Proc. Roy. Soc.* **87**, 277 (1912).
14. C. T. R. Wilson, "Investigation on X-rays and Beta-rays by the Cloud Method," *Proc. Roy. Soc.*, **104**(1), 192 (1923).
15. H. Fujita, "Studies on Atom Clusters by Ultra-high Voltage Electron Microscopy," Materials Transactions, JIM, **35**(9), 563-575 (1994).
16. H. Fujita, "Usefulness and Applications of Electron Microscopy to Materials Science," *Materials Transactions*, JIM, **31**(7), 523-537 (1990).
17. H. Fujita, "Atom Clusters-new Applications of High Voltage Electron Microscopy Micro-laboratory to Materials Science," *Ultramicroscopy*, **39**, 369-381 (1991).
18. N. M. Hwang and D. Y. Yoon, "Driving Force for Deposition in the Chemical Vapor Deposition Process," *J. Mater. Sci. Let.*, **13**, 1437-1439 (1994).
19. G. Garcia, J. Casado, J. Libre and A. Figueras, "Preparation of YSZ Layers by MOCVD: Influence of Experimental Parameters on the Morphology of the Films," *J. Crystal Growth*, **156**. 426-432 (1995).
20. E. T. Kim. J. W. Lee, S. H. Lee and S. G. Yoon, "Characterization of Y_2O_3-Stabilized ZrO_2 Thin Films by Plasma-Enhenced Metallorganic Chemical Vapor Deposition," *J. Electrochem. Soc.*, **140**(9), 2625-2629 (1993).
21. L. Ben-Dor, A. Elshtein, S. Halashi, I. Pinsky and J. Shappir, "Thin Films of ZrO_2 Metal Organic Chemical Vapor Deposition," *J. Electronic Materials* **13**(2), 263-272 (1984).
22. E. T. Kim and S.G. Yoon, "Characterization of Zirconium Dioxide Film Formed by Plasma-Enhenced Metall-organic Chemical Vapor Deposition," *Thin Soild Film*, **227**, 7-12 (1993).